RESEARCH



Cell phone microscopy enabled low-cost manufacturable colorimetric urine glucose test

Zhuolun Meng¹ · Hassan Raji¹ · Muhammad Tayyab¹ · Mehdi Javanmard¹

Accepted: 24 October 2023 / Published online: 6 November 2023 © The Author(s), under exclusive licence to Springer Science+Business Media, LLC, part of Springer Nature 2023

Abstract

Glucose serves as a pivotal biomarker crucial for the monitoring and diagnosis of a spectrum of medical conditions, encompassing hypoglycemia, hyperglycemia, and diabetes, all of which may precipitate severe clinical manifestations in individuals. As a result, there is a growing demand within the medical domain for the development of rapid, cost-effective, and userfriendly diagnostic tools. In this research article, we introduce an innovative glucose sensor that relies on microfluidic devices meticulously crafted from disposable, medical-grade tapes. These devices incorporate glucose urine analysis strips securely affixed to microscope glass slides. The microfluidic channels are intricately created through laser cutting, representing a departure from traditional cleanroom techniques. This approach streamlines production processes, enhances cost-efficiency, and obviates the need for specialized equipment. Subsequent to the absorption of the target solution, the disposable device is enclosed within a 3D-printed housing. Image capture is seamlessly facilitated through the use of a smartphone camera for subsequent colorimetric analysis. Our study adeptly demonstrates the glucose sensor's capability to accurately quantify glucose concentrations within sucrose solutions. This is achieved by employing an exponential regression model, elucidating the intricate relationship between glucose concentrations and average RGB (Red-Green-Blue) values. Furthermore, our comprehensive analysis reveals minimal variation in sensor performance across different instances. Significantly, this study underscores the potential adaptability and versatility of our solution for a wide array of assay types and smartphone-based sensor systems, making it particularly promising for deployment in resource-constrained settings and undeveloped countries. The robust correlation established between glucose concentrations and average RGB values, substantiated by an impressive R-square value of 0.98709, underscores the effectiveness and reliability of our pioneering approach within the medical field.

Keyword Disposable devices · Easy fabrication · Medical tape · Rapid glucose testing · Smartphone colorimetric measurement

1 Introduction

Glucose, often referred to as blood sugar, serves as the primary energy source for the body's cells. It is transported via the bloodstream and serves as the vital fuel for cells

Mehdi Javanmard mehdi.javanmard@rutgers.edu

Zhuolun Meng zhuolun.meng@rutgers.edu

Hassan Raji hassan.raji@rutgers.edu

Muhammad Tayyab muhammad.tayyab@rutgers.edu

Electrical and Computer Engineering, Rutgers University-New Brunswick, 94 Brett Road, Piscataway 08854, New Jersey, USA throughout the human body, particularly for the brain, nervous system, and muscles. However, when glucose levels become elevated, a condition known as hyperglycemia can develop, which is closely linked to conditions such as diabetes, stress, illness, and certain medications. Conversely, when glucose levels plummet to abnormally low levels, it can lead to hypoglycemia, a state associated with potential complications, including cognitive impairment, cardiovascular diseases, and nerve damage. Therefore, the maintenance of a healthy glucose level is paramount for overall health (Blood Sugar Blood Glucose Diabetes 2023; Blood Glucose (Sugar) Test 2022). According to data from the Centers for Disease Control and Prevention (CDC), the United States currently reports 37.3 million diagnosed cases of diabetes, accompanied by an additional 96 million adults aged 18 years or older who exhibit prediabetic conditions. This prevalence corresponds to a substantial 38% of the adult



American population (National Diabetes Statistics Report 2022). In 2017, the United States allocated a staggering 327 billion USD toward the management and treatment of diabetes and its related comorbidities, underscoring the significant financial impact of this disease burden (Zhou et al. 2016; Zhang et al. 2022).

With the development of microfluidic devices and biosensors in the past few decades, there has been rapid growth in biomedical sensors that satisfy the ASSURED criteria (Affordable, Sensitive, Specific, User-friendly, Rapid and Robust, Equipment-free, and Deliverable) for analytical chemistry and medical detection (Drummond et al. 2003; Kamholz et al. 1999; Kim and Park 2005; Whitesides 2006; Dittrich et al. 2006; Reyes et al. 2006; Mahmoodi et al. 2021; Mok et al. 2014; Huang et al. 2012). However, despite the maturity of current techniques for making biosensors and microfluidic devices, there are still some unavoidable defects, such as significant time and effort for both design and fabrication, and the cleanroom environment, materials, and skilled operators all being expensive. This has led numerous researchers and scientists continue shifting their focus towards microfabrication aspects (Piyasena and Graves 2014; Tania et al. 2020; Weibel et al. 2007; Lin et al. 2020; Sui et al. 2020; Sui et al. 2020; Tayyab et al. 2022; Xie et al. 2020; Guo and Ma 2017; Zhao et al. 2020).

To compensate for the limitations of silicon fabrication, soft microfluidic channels have been explored due to their use of elastomers, which are relatively inexpensive, transparent, inert, biocompatible, easy to fabricate and fast to fabricate. Nevertheless, the bonding encountered during PolyDimethylSiloaxane (PDMS) channels can be challenging (Chow et al. 2005; El-Ali et al. 2006; Quake and Scherer 2000; Abate et al. 2008; Duffy et al. 1998; Iliescu et al. 2012; Zhang et al. 2022). Baking or oxide plasma is required to assemble PDMS channels onto other substrates. Additionally, PDMS takes a long time to solidify and the quality is hard to control, making it difficult to eliminate bubbles completely. Furthermore, masks are still needed to realize the expected shapes, which are not always flexible.

In recent years, disposable devices have become highly desirable in the biosensor field due to their low risk of mutual contamination, disposability, point-of-care, ease of fabrication, low cost, and fast fabrication, which makes them as a perfect candidate for use in the diagnosis area (Yager et al. 2006; Yu et al. 2008; Zhang et al. 2010; Cho et al. 2017; Eletxigerra et al. 2015; Fiorini and Chiu 2005; Xia et al. 2016; Meng et al. 2022; Meng et al. 2022; Huang et al. 2019). In this paper, we describe an alternative approach for fabricating glucose sensors using medical-grade tapes and analysis strips which satisfy all of these advantages (Tania et al. 2020; Meng et al. 2022; Meng et al. 2022). We illustrate the design, fabrication process and assembly procedure of a glucose diagnostic sensor using colorimetric measurement based

on a smartphone camera and average RGB measurement algorithm (Tania et al. 2020; Meng et al. 2022; Meng et al. 2022; Wang et al. 2010; Kim et al. 2017; Mei et al. 2016). We addressed the issue that the color change of glucose strips is difficult to recognize visually by implementing a 3D-printed, detachable and flexible phone housing to eliminate outside illumination effects (Meng et al. 2022; Meng et al. 2022; Smith et al. 2016; Talebian and Javanmard 2021). In comparison to the methods discussed in Xia et al review paper (Xia et al. 2016), our sensor achieves improved accuracy through meticulous control of the illumination background Smith et al. (2016). Unlike similar approaches (Jalal et al. 2017; Kanakasabapathy et al. 2017), our solution stands out for its exceptional flexibility, making it suitable for a wide range of assays and contexts. The laser-cut channels can be easily reshaped to align with the dimensions and shapes of various substrates. The regression models we obtained from titration experiments of multiple glucose concentrations show an exponential relationship between glucose concentrations and average RGB values, and a comparison between bare original strips and our glucose sensor shows that our glucose sensor is a better alternative.

2 Methods and Materials

2.1 Microfluidic device fabrication

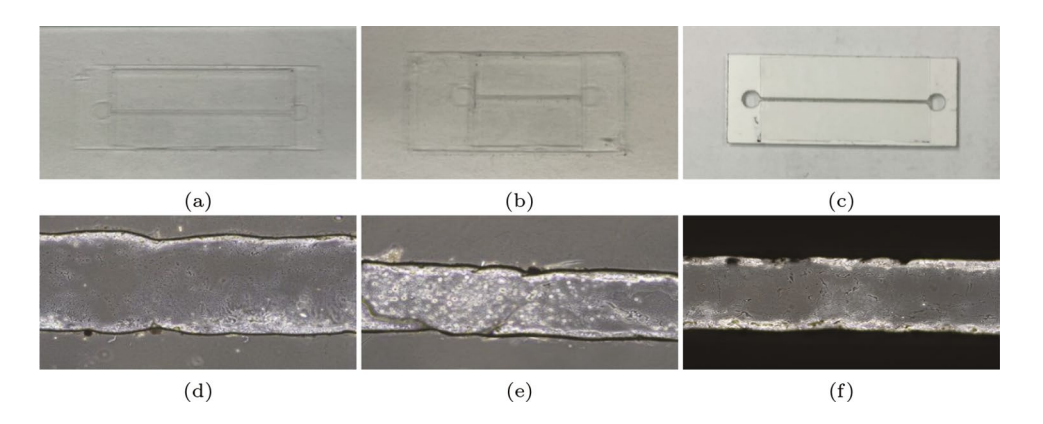
The microfluidic channel was fabricated utilizing two medical-grade tapes. The two double-sided adhesive tapes (3M 9965/9969 Diagnostic Microfluidics tape, 3M, MN, USA) were engraved using a laser cutter (Boss LS1420, MinPower (%)-1: 14, Max-Power (%)-1: 14, Speed(mm/s): 9, Boss Laser, FL, USA) to create the main structure of microfluidic channels. The 2D modeling design of the microfluidic channels was completed on AutoCAD. The glucose analysis strip (ACCUTEST Urine Reagent Strip, Accutest, CA, USA) was placed into the main channel structure, which was covered and sealed by a thin layer of glass slide. Compared to other similar approaches, this solution offers greater flexibility for application in various assays and contexts. For instance, the substrate materials can be easily switched to accommodate the user's specific needs, thanks to the ability to design and fabricate custom-shaped microfluidic channels using Auto-CAD and a laser cutter. Furthermore, these devices can be easily mass-produced at a low cost.

In Fig. 1, the three images show the actual microfludic devices fabricated in both 3D 9965 and 9969 tapes, while the bottom three images are microscopic photos of the three microfludic channels.

The engraved medical-grade tapes were placed onto the base of microscope glass slides (AmScope, United Scope



Fig. 1 a, b, c Real photos of three devices different lengths (22, 11, 22 mm), thickness (25, 25, 86 um), and width (200, 100, 200 um). d, e, f Microscopic photos corresponding to the above three devices



LLC., CA, USA) due to their accessibility and cost-effectiveness. However, the substrate can be easily switched according to users' real-life situations, thanks to the flexibility of this solution. To ensure the proper assembly of the microfluidic device, it is crucial to carefully position the thin glass slides onto the channel and use spudgers to eliminate any bubbles between the medical-grade tapes and thin glass slides. It is essential to move the spudgers in one direction and be cautious not to apply excessive pressure when pressing the glass slides and tape together. After assembly, the microfluidic devices should be baked at 80°C for 30 seconds in an oven to enhance adhesion between the tape and glass slides and prevent any gaps, even in the presence of contamination.

In Fig. 2(a) and (b), two microfluidic devices were fabricated using 3M 9965 and 9969 tapes, with the same dimensions expect for the thickness (3D 9965: thickness is 86 μ m and 3D 9969: thickness is 25 μ m). These two devices were able to hold and transport the dyed Phosphate-buffered saline (PBS) perfectly, with no leakage problems. It is important to handle the device carefully throughout the assembly process to avoid damage and to prevent the introduction of contaminants that could affect its performance. Our glucose sensors were made from the microfluidic channels, and the glucose testing strips (ACCUTEST Urine Reagent Strip, Accutest, CA, USA) were placed into the channels, as shown in Fig. 2(c). Two layers of tape were stacked to increase the in-channel space, accommodating the thickness of glucose analysis strips for glucose sensors. The

glucose strips were placed at the end of the channels because any color change caused by the reaction between glucose and analysis strips will be carried forward in the channels which would introduce errors in this method.

2.2 Hardware components

The hardware used for the glucose measurement platform is a customized 3D-printed housing that holds the glucose sensors. The housing was designed using AutoCAD and 3D printed using Ultimaker S5 3D printer and Ultimaker Polylacticacid (PLA) as filament material (Ultimaker, Utrecht, Netherlands). An iPhone 12 (Apple, Inc., Cupertino, CA, USA) is utilized as the primary smartphone camera to complete all experiments. The 3D-printed housing is a black opaque box that blocks outside light noise and illumination variations that can fluctuate with different environments (Meng et al. 2022; Meng et al. 2022; Smith et al. 2016). Notably, the microfluidic channel extends beyond the box for easy sample loading. Each side of the housing was 3D printed individually and assembled via interlocking cutouts shown in Fig. 3(a). These cutouts allow the box to be easily disassembled and reassembled, and the box can be packaged in individual pieces, making it easier to store and ship. In Fig. 3(b), the cross-sectional view of this housing is shown (size: $279 \times 179 \times 100$ mm). Additionally, two methods were used to eliminate the outside light noise. First, coarse sandpaper (150 grit) was used to sand the bottom part to

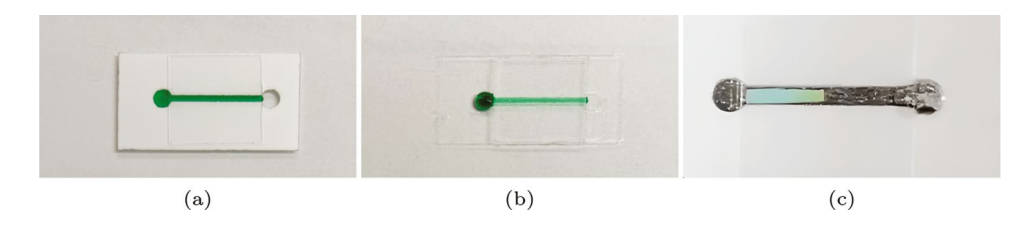


Fig. 2 a Microfluidic device made by 3M 9965 medical-grade tape with no leakage transportation of dyed PBS solution (Thickness: 86 μ m). b Microfluidic device made by 3M 9969 medical-grade tape

with no leakage transportation of dyed PBS solution (Thickness: $25 \mu m$). c Glucose sensor made by 3M 9965 medical-grade tape with no leakage transportation of sucrose solution (Thickness: $172 \mu m$)



13 Page 4 of 10 Biomedical Microdevices (2023) 25:43

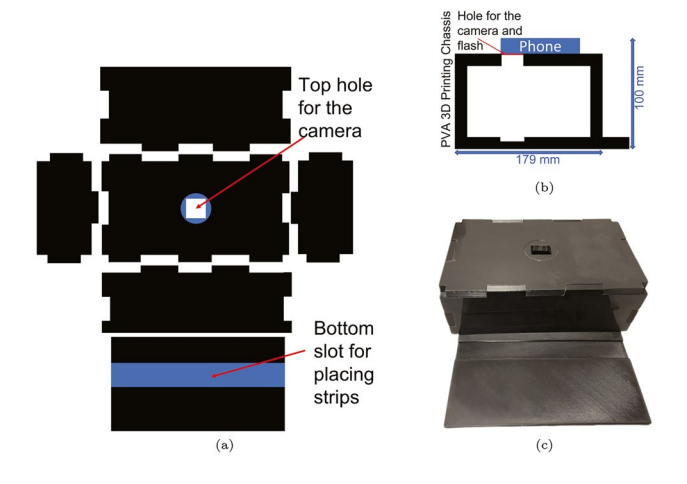


Fig. 3 a Six individual interlocking 3D printed parts. b Cross-sectional view of housing. c Real 3D printed housing with sand bottom part and within a slot for samples. (size: $279 \times 179 \times 100$ mm)

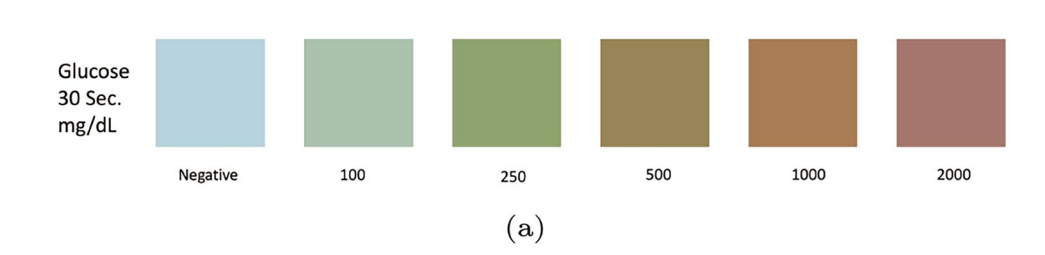
absorb light and reduce reflection. Second, the top cover's hole was designed separately and can be replaced to fit various camera shapes and eliminate outside lights.

2.3 Glucose measurement algorithm

To quantitively measure the colorimetric values of the glucose sensors using glucose analysis strips as biomarker, the average RGB value was selected as the parameter to represent the concentration of glucose for glucose test strips measurements. According to the user manual of glucose analysis strips, the color of the reacted analysis strips will shift from light green to dark red with the increase of glucose concentrations shown in Fig. 4.

The enzyme glucose oxidase catalyzes the formation of gluconic acid and hydrogen peroxide through the oxidation of glucose. Hydrogen peroxide, in turn, triggers the release of neoelectrocytes oxide [O] through the action of peroxidase. This oxide [O] oxidizes potassium iodide, leading to a change in color. Thus, the algorithm used was avg RGB=(R+G+B)/3, which combines the red, green, and blue channels and interprets the inverse proportional relationship between average RGB values and glucose concentrations. The ImageJ tool was implemented to measure the colorimetric values.

Fig. 4 Glucose analysis strip reading activity





3 Results

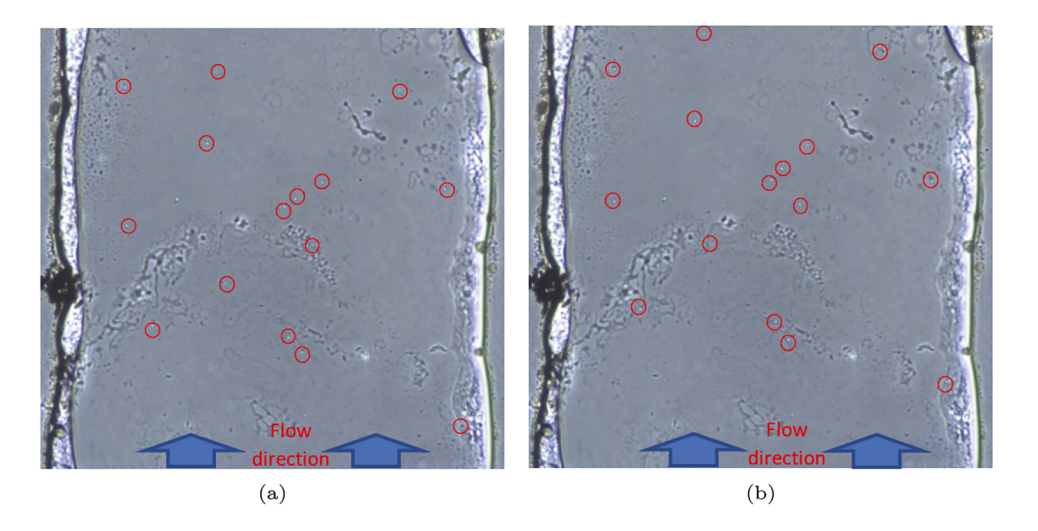
3.1 Characterization of microfluidic channel

In order to evaluate the flow velocity responses of diverse channels with different dimensions (25, 50, 86 µm height, 11, 22 mm length, and 300, 500, 700 µm width), Streptavidin Polystyrene microbeads with a diameter of 3.23 µm (Spherotech Inc., Lake Forest, IL, USA) were injected into the microfludic channels as a reference for flow. This characterization elucidates the fundamental attributes of this microfludic device, serving as a valuable reference for future users in diverse applications.

This versatility in biomedical devices opens doors to its integration in various assays or impedance cytometry as demonstrated in prior work (Lin et al. 2023). The experiments were conducted using a Nikon Eclipse Ts2 microscope (Nikon Instruments Inc., Melville, NY, USA). A range of channels were fixed under microscope, and videos were recorded to capture the motion of as many microbeads as possible within the range. The velocities of the beads were obtained by measuring the frames split from the videos. The channels were oriented vertically, so the flow direction was upward in the images shown in Fig. 5 (Gholizadeh and Javanmard 2016).

In Fig. 6, six groups of comparison are shown to investigate the effect of dimensions on flow velocities using the controlled variates method. This method fixes two parameters of length, width and height of channels while changing the rest as a variate. Overall, the plots show that the velocities decrease over time. From Fig. 5, the results show that the heights of the microfluidic channels have a significant impact on the initial flow velocity, which then merge into similar velocities after 100 seconds, and the higher channels will slow down the flow velocities. Longer microfludic channels result in slower velocities, while narrower microfludic channels also lead to slower velocities. Thus, with a larger height and length, the flow velocities will be smaller because the inside space is larger, and under same volume injection, a larger flow area will direct lower speed. However, the channel width is the opposite, as narrow channels will suppress the liquid to non-smooth flow, decreasing the flow speed.

Fig. 5 Capture of a microfluidic channel with 25 um height, 300 um width, and 11 mm length a Beads positions for initial frame. b Beads positions after 2 seconds moving



The prediction of this characterization is that the flow speed will slow down as one parameter, such as length, width, or height, increases while the others are held constant. For instance, under the same length and width conditions, the flow speed will decrease with a larger channel height. However, curves resembling a ping-pong shape, as seen in the orange curve in Fig. 6(b) and the green curve in Fig. 6(d), are

observed. These shapes are attributed to the working principle of the laser cutter. The channel edges are not perfectly smooth, leading to discontinuous liquid flow inside the microfluidic channels due to capillary breaks at different points within the channels. The frames were captured during static flow or when the flow exhibited random movement, coincidentally resulting in ping-pong shapes. The measured velocities that do not

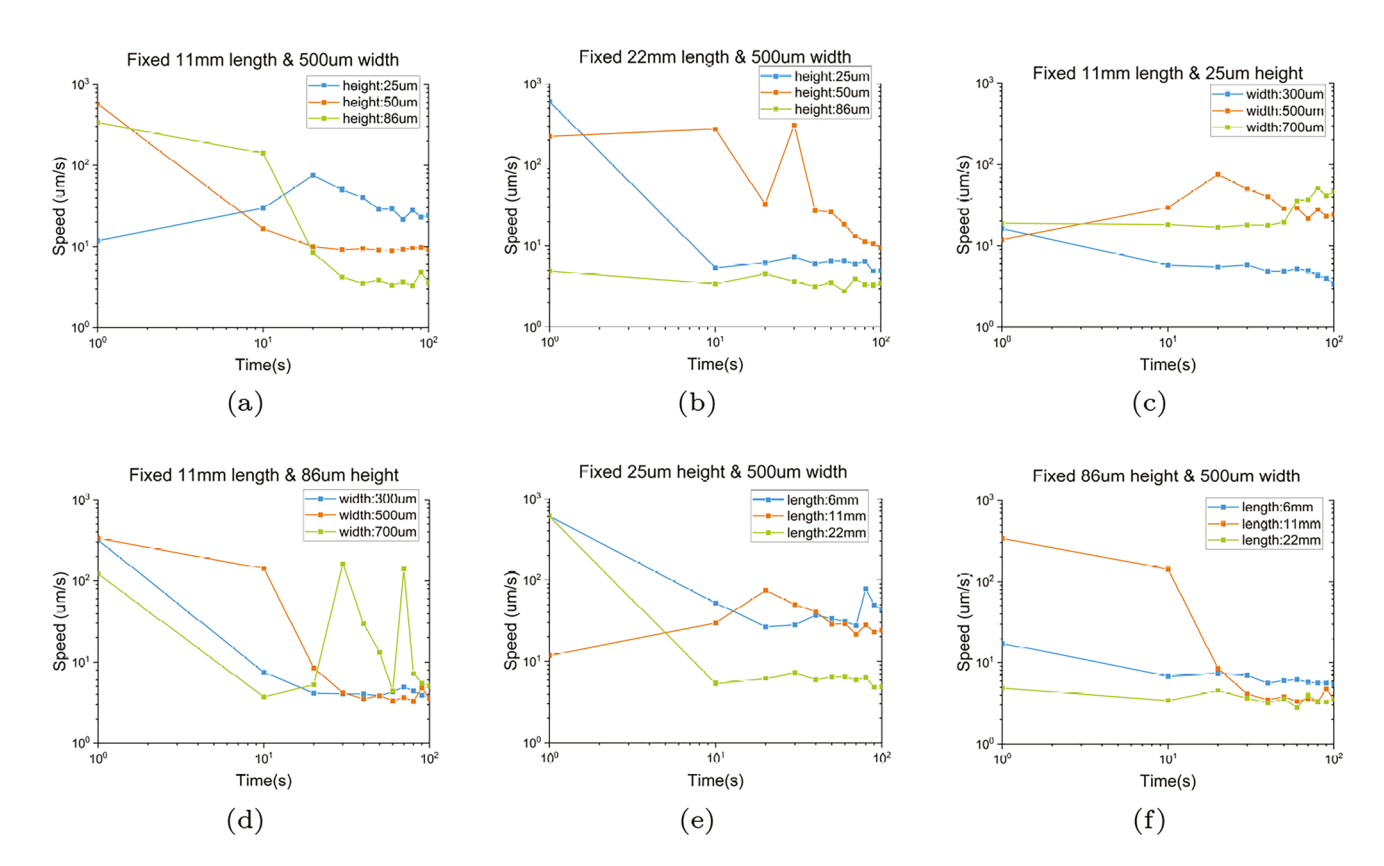


Fig. 6 Compared plots showing the dimensions affects. $\bf a$ and $\bf b$ Fixed length (11 & 22 mm) and width (500 um), different heights (25, 50, 86 um). $\bf c$ and $\bf d$ Fixed length (11 mm) and height (25 & 86 um), dif-

ferent widths (300, 500, 700 um). $\bf e$ and $\bf f$ Fixed width (500 um) and height (25 & 86 um), different lengths (6, 11, 22 mm)



Fig. 7 a In-channel strip before pipetting glucose. **b** In-channel strip after 3 mins of glucose pipetting



align with the expected predictions are attributed to the fact that velocities were measured and calculated by observing microbeads inside the channels. This method can exaggerate the irregularities in the microfluidic channels created by the laser cutter. Nevertheless, the velocities still conform to the predictions on a macro scale

3.2 Characterization of glucose sensor

The device's scalability in manufacturing and flexibility in the substrate material selection are its key strengths. This type of glucose sensor can easily adapt to various substrate dimensions, enabling efficient and cost-effective production. Furthermore, the utilization of affordable assay test strips makes our sensor an economical diagnostic method adaptable to diverse assays such as potassium, sodium, and hemoglobin. Such inexpensive assays hold great potential for use in resource-constrained developing countries. The retail price for one sensor stands at \$0.24 USD. With bulk production, the estimated cost can decrease to as low as \$0.19 USD per sensor for large orders or even lower.

The performance of glucose sensor was characterized through comparative experiments between our glucose sensor (in-channel strips) and original bare glucose test strips (out-channel strips). Fig. 7(a) shows the start of pipetting the sucrose solution into the in-channel strip, and Fig. 7(b) shows the picture after 3 mintues of reaction with an obvious color change.

To calibrate the standard of our glucose sensor, the comparative experiments between in-channel and out-channel glucose sensors were conducted. To obtain titration curves for both in-channel and out-channel sensores, different glucose concentrations were measured by the glucometer (ANKOVO TD-4627, Shenzhen, China), and were plotted against the average RGB values of the glucose sensors obtained using ImageJ. Titration experiments were performed at six concentrations: 0, 100, 250, 500, 1000 and more than 2000 mg/dL, which correspond to the turning points of color change indicated in the color chart provided by the supplier.

Figure 8 shows that the in-channel sensors had a slower reaction time than the out-channel strips but similar average RGB values for all six concentrations. However, the in-channel sensors consumed much less solution (5 μ L) than the out-channel strips (20 μ L) because the surface of the glucose testing strip are hydrophobic,

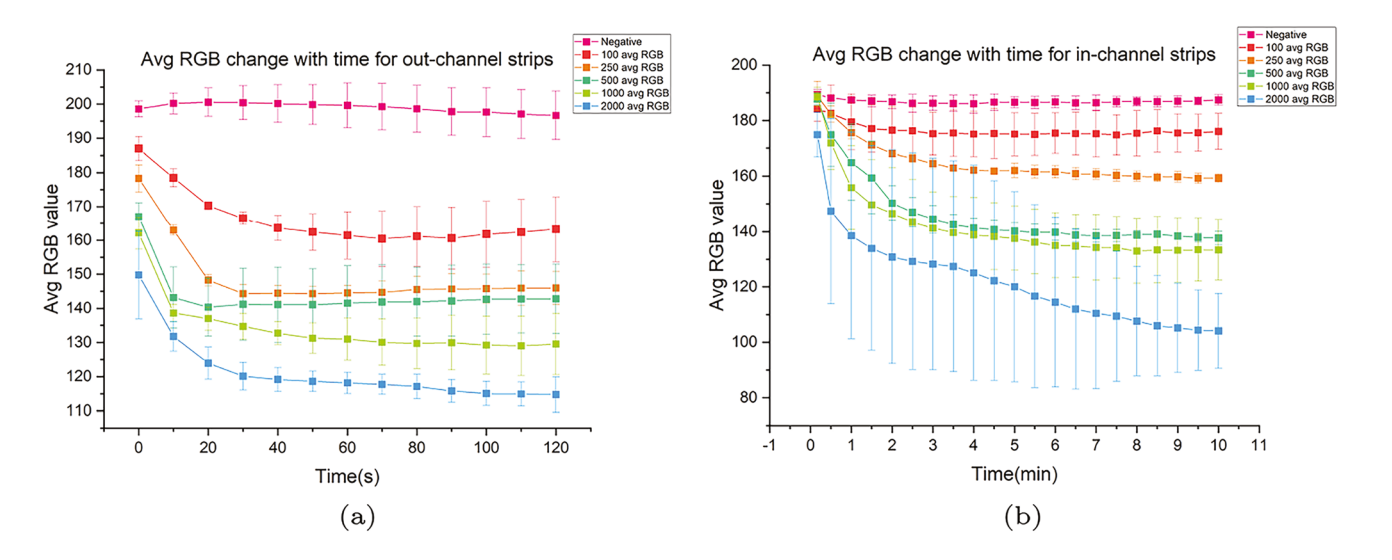
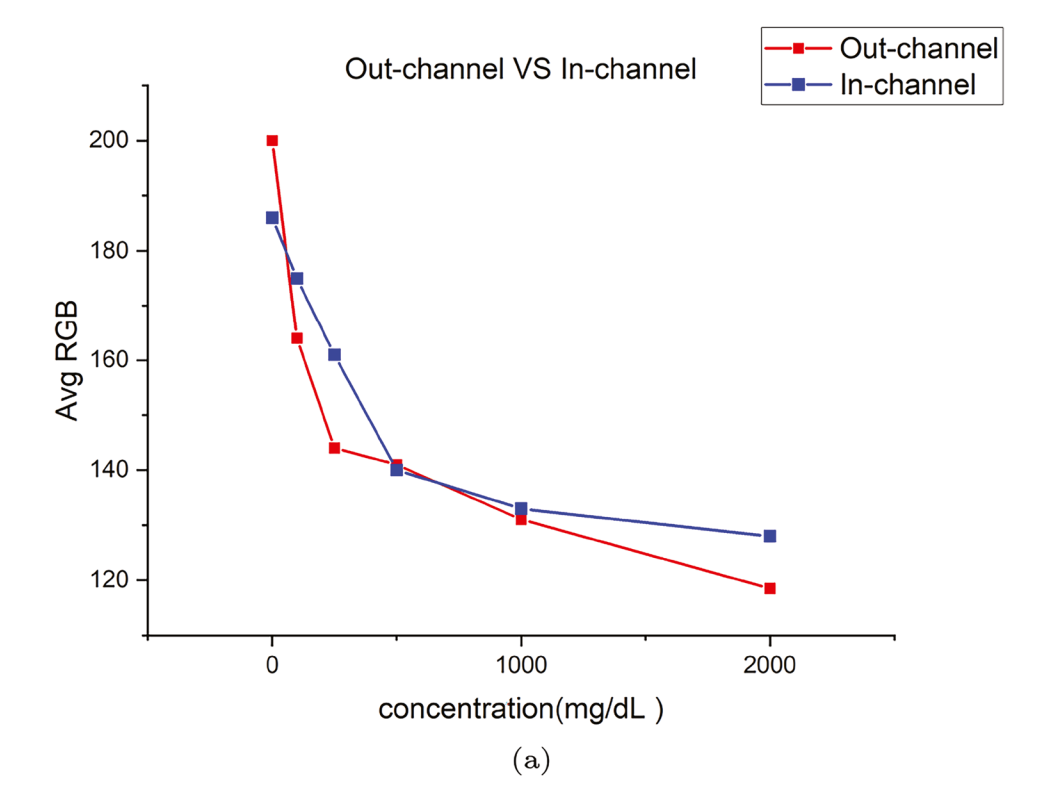


Fig. 8 a Color change with time on out-channel strips. b Color changes with time on in-channel strips



Fig. 9 Comparison of the Relationship between Glucose Concentration and Average RGB Values in Original Glucose Analysis Strips (Out-channel) and Our Glucose Sensor (Inchannel)



making it difficult to absorb the solution. In Fig. 8(b), the error bar for 2000 mg/ dL is large due to the different absorbance rates of the different strips, but the final RGB values are similar.

In Fig. 9, we compared the titration curves of both the original strips and the glucose sensors. We calculated the mean values using the average RGB values from the flat and steady portions of the curves in Fig. 8. To ensure accurate readings and sufficient reaction time, we selected an average range between 30 to 50 seconds for out-channel strips and 4 to 5 minutes for in-channel strips. In Fig. 9, it is evident that the blue curve exhibits less curvature than the red curve. This observation indicates that, for glucose concentrations both below and above 500 mg/dL, the glucose sensors produce smaller average RGB values compared to the original glucose analysis strips. The average RGB value for the original strips exceeds that of the glucose sensor only when the solution is pure PBS. Although the two curves do not entirely overlap, they follow similar trends, confirming that the glucose sensor consistently generates comparable reaction results to the original glucose analysis strips. This consistency demonstrates its suitability for substitution. For this type of glucose sensor, the timing is crucial, as prolonged exposure can lead to less reliable diagnostic results. Additionally, variations in diagnostic values can occur due to different brands of analysis strips and various smartphone models. Ultimately, if the sensor is adopted by users employing a range of analysis strips and smartphone models, each combination may require a custom-designed phone holder and calibration for image response. This is because each camera model exhibits unique characteristics.

In Fig. 10, the results show exponential relationships between glucose concentrations and the average RGB values, and the functions are Y=126.28 + 71.39*exp(-0.00575*X) and Y=120.88 + 65.84*exp(-0.00217*X) for out-channel and in-channel strips, respectively. The R-square numbers are 0.95902 and 0.98709 for out-channel and in-channel, respectively.

In this section, we have exclusively tested the sucrose solution as it aligns with the primary focus of describing our fundamental methodology and algorithm in this article. When dealing with urine samples, new calibrations will be necessary for image processing. Ultimately, the complete testing of urine samples will be performed fully to demonstrate the universality of this glucose sensor and recalibration for image response will be essential for its image response in the future, considering the differences between urine samples and the sucrose solution.



43 Page 8 of 10 Biomedical Microdevices (2023) 25:43

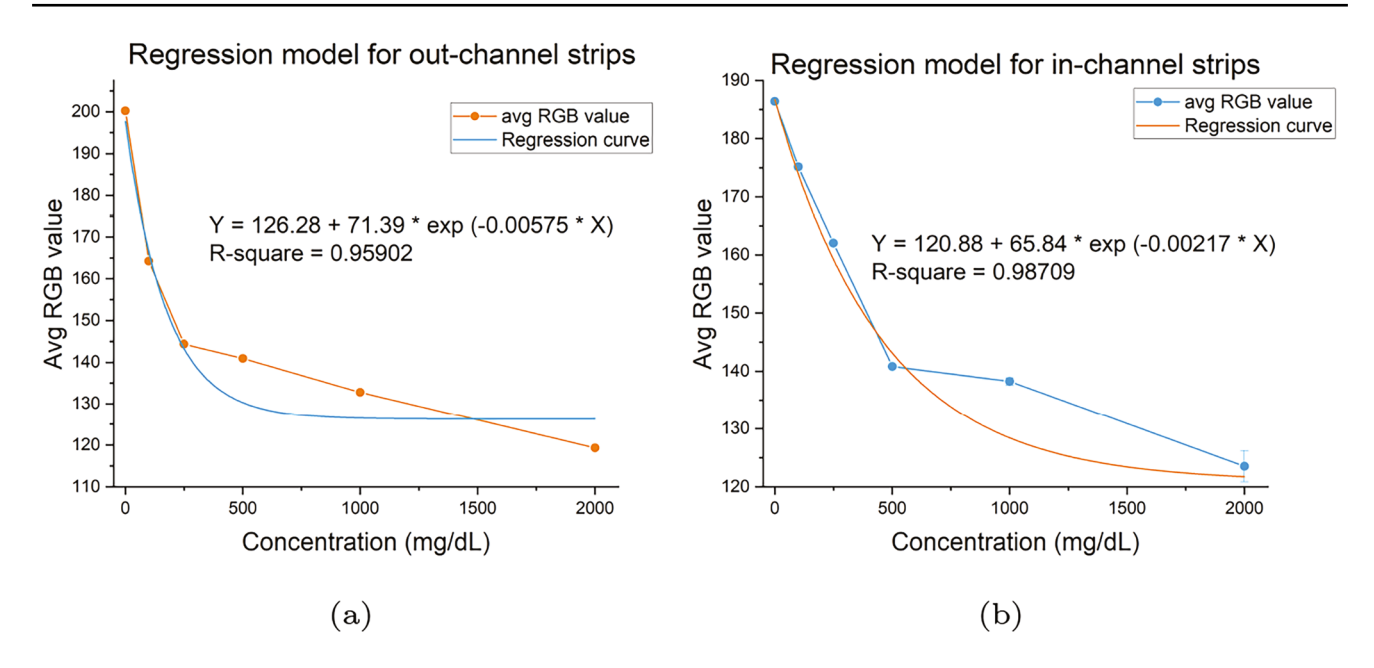


Fig. 10 a Regression model for out-channel strips. b Regression model for in-channel strips

4 Conclusion

In this paper, we present a novel microfluidic device fabricated using disposable and medical-grade tapes and glass slides, which can compensate for defects in microfabrication devices and PDMS microfluidic channels. Our fabrication method is uncomplicated, flexible, economical and disposable, making it a suitable solution for society's extreme requirements. The cost of one chip can be lowered to \$0.24. The 3D-printed black opaque housing improves light control and blocks all outside lighting noise. Additionally, compared to naked-eye observation, our algorithm provides a more accurate and easy way to measure the glucose levels in the solution through the average RGB values. This method can be transplanted to portable smartphones, providing direct measurement results in the near future.

Due to the controllable ability of shapes and flow velocities of the microfluidic channels, this device can be extended to comprehensive diagnosis areas. The results presented in this paper illustrate fundamental research and feasibility using medical-grade tapes as disposable glucose sensors. We tested one phone model as it describes the methodology and algorithm using the average RGB values, which is independent of phone models. For future work, if and when this device is used by various smartphone models and cameras, each different phone model will require its own top hole design on the top of housing and will need to be recalibrated for its image response, as every camera model differs from another. The scope of this paper was fundamental research and demonstrating feasibility rather

than showing universality across all smartphone models. Finally, the regression curves were given by different concentrations of glucose with 0.959 and 0.987 R-Square, which demonstrate the confidence of our glucose sensors and related regression model.

PDMS is more difficult and costly to manufacture with scalability and transferability than medical-grade tapes. Our device boasts scalable manufacturability and substrate material flexibility, setting it apart from current microfluidics-based technology. Each device costs approximately \$0.24 USD, with the potential to drop to as low as \$0.19 USD when produced in bulk with favorable raw material pricing. This cost is comparable to commercial glucometer test kits, making it an economical choice. Unlike traditional glucometers, our solution leverages consumer electronics, eliminating the need for users to purchase a separate glucometer device. The use of a laser cutter to create channels enables easy scaling to accommodate various substrate dimensions, streamlining manufacturing and reducing costs. Furthermore, our device is compatible with a range of sterile substrate materials, offering producers the flexibility to utilize readily available resources. Our device's strong transferability is a standout feature, thanks to its adaptable manufacturing methods. It can be effortlessly redesigned to suit different assay types and smartphone interfaces, enhancing its versatility for both users and manufacturers. In summary, the combination of scalable manufacturability, strong transferability, and cost-effectiveness positions our device as an adaptable and valuable solution for a wide range of applications.



Acknowledgements This work was supported in part by the National Science Foundation under Grant 1711165, 1556253 and 1846740.

Author contributions M.J. and Z.M. conceived the project. Z.M. performed experiments with help from H.R. and M.T.. Z.M. wrote the paper with review of M.J., H.R., and M.T.

Funding This work was supported in part by the National Science Foundation under Grant 1711165, 1556253 and 1846740.

Data availability All study data are included in the article.

Declarations

Ethical approval Not applicable.

Competing interests The authors declare no competing interests.

References

- A.R. Abate, D. Lee, T. Do, C. Holtze, D.A. Weitz, Glass coating for pdms microfluidic channels by sol-gel methods. Lab Chip 8(4), 516–518 (2008)
- Blood Glucose (Sugar) Test: Levels & What They mean. (2022). https://my.clevelandclinic.org/health/diagnostics/12363-blood-glucose-test
- Blood Sugar Blood Glucose Diabetes. U.S. National Library of Medicine. (2023). https://medlineplus.gov/bloodglucose.html
- H. Cho, J. Kim, C.-W. Jeon, K.-H. Han, A disposable microfluidic device with a reusable magnetophoretic functional substrate for isolation of circulating tumor cells. Lab Chip 17(23), 4113–4123 (2017)
- W.W.Y. Chow, K.F. Lei, G. Shi, W.J. Li, Q. Huang, Microfluidic channel fabrication by pdms-interface bonding. Smart Mater. Struct. 15(1), 112 (2005)
- P.S. Dittrich, K. Tachikawa, A. Manz, Micro total analysis systems. latest advancements and trends. Anal. Chem. 78(12), 3887–3908 (2006)
- T.G. Drummond, M.G. Hill, J.K. Barton, Electrochemical dna sensors. Nat. Biotechnol. 21(10), 1192–1199 (2003)
- D.C. Duffy, J.C. McDonald, O.J. Schueller, G.M. Whitesides, Rapid prototyping of microfluidic systems in poly (dimethylsiloxane). Anal. Chem. 70(23), 4974–4984 (1998)
- J. El-Ali, P.K. Sorger, K.F. Jensen, Cells on chips. Nature 442(7101), 403–411 (2006)
- U. Eletxigerra, J. Martinez-Perdiguero, S. Merino, Disposable microfluidic immuno-biochip for rapid electrochemical detection of tumor necrosis factor alpha biomarker. Sens. Actuators B Chem. 221, 1406–1411 (2015)
- G.S. Fiorini, D.T. Chiu, Disposable microfluidic devices: fabrication, function, and application. BioTechniques 38(3), 429–446 (2005)
- A. Gholizadeh, M. Javanmard, Magnetically actuated microfluidic transistors: Miniaturized micro-valves using magnetorheological fluids integrated with elastomeric membranes. J. Microelectromechanical Syst. 25(5), 922–928 (2016)
- J. Guo, X. Ma, Simultaneous monitoring of glucose and uric acid on a single test strip with dual channels. Biosens. Bioelectron. 94, 415–419 (2017)
- Z. Huang, X. Li, M. Martins-Green, Y. Liu, Microfabrication of cylindrical microfluidic channel networks for microvascular research. Biomed. Microdevices 14, 873–883 (2012)
- X. Huang, Y. Li, J. Chen, J. Liu, R. Wang, X. Xu, J. Yao, J. Guo, Smartphone-based blood lipid data acquisition for cardiovascular disease management in internet of medical things. IEEE Access 7, 75276–75283 (2019)

- C. Iliescu, H. Taylor, M. Avram, J. Miao, S. Franssila, A practical guide for the fabrication of microfluidic devices using glass and silicon. Biomicrofluidics 6(1), 016505 (2012)
- U.M. Jalal, G.J. Jin, J.S. Shim, Paper-plastic hybrid microfluidic device for smartphone-based colorimetric analysis of urine. Anal. Chem. 89(24), 13160–13166 (2017)
- A.E. Kamholz, B.H. Weigl, B.A. Finlayson, P. Yager, Quantitative analysis of molecular interaction in a microfluidic channel: the t-sensor. Anal. Chem. 71(23), 5340–5347 (1999)
- M.K. Kanakasabapathy, M. Sadasivam, A. Singh, C. Preston, P. Thirumalaraju, M. Venkataraman, C.L. Bormann, M.S. Draz, J.C. Petrozza, H. Shafiee, An automated smartphone-based diagnostic assay for point-of-care semen analysis. Sci. Transl. Med. 9(382), 7863 (2017)
- K.S. Kim, J.-K. Park, Magnetic force-based multiplexed immunoassay using superparamagnetic nanoparticles in microfluidic channel. Lab Chip 5(6), 657–664 (2005)
- S.C. Kim, U.M. Jalal, S.B. Im, S. Ko, J.S. Shim, A smartphone-based optical platform for colorimetric analysis of microfluidic device. Sens. Actuators B Chem. 239, 52–59 (2017)
- Z. Lin, S.-Y. Lin, P. Xie, C.-Y. Lin, G.M. Rather, J.R. Bertino, M. Javanmard, Rapid assessment of surface markers on cancer cells using immuno-magnetic separation and multi-frequency impedance cytometry for targeted therapy. Sci. Rep. 10(1), 3015 (2020)
- Z. Lin, J. Sui, M. Javanmard, A two-minute assay for electronic quantification of antibodies in saliva enabled through a reusable microfluidic multi-frequency impedance cytometer and machine learning analysis. Biomed. Microdevices 25(2), 13 (2023)
- S.R. Mahmoodi, P. Xie, D.P. Zachs, E.J. Peterson, R.S. Graham, C.R. Kaiser, H.H. Lim, M.G. Allen, M. Javanmard, Single-step label-free nanowell immunoassay accurately quantifies serum stress hormones within minutes. Sci. Adv. **7**(27), 4401 (2021)
- Q. Mei, H. Jing, Y. Li, W. Yisibashaer, J. Chen, B.N. Li, Y. Zhang, Smartphone based visual and quantitative assays on upconversional paper sensor. Biosens. Bioelectron. 75, 427–432 (2016)
- Z. Meng, M. Tayyab, Z. Lin, H. Raji, M. Javanmard, A smartphone-based disposable hemoglobin sensor based on colorimetric analysis. Sensors 23(1), 394 (2022)
- Z. Meng, A. Williams, P. Liau, T.G. Stephens, C. Drury, E.N. Chiles, X. Su, M. Javanmard, D. Bhattacharya, Development of a portable toolkit to diagnose coral thermal stress. Sci. Rep. 12(1), 14398 (2022)
- J. Mok, M.N. Mindrinos, R.W. Davis, M. Javanmard, Digital microfluidic assay for protein detection. Proc. Natl. Acad. Sci. 111(6), 2110–2115 (2014)
- National Diabetes Statistics Report. Centers for Disease Control and Prevention (2022). https://www.cdc.gov/diabetes/data/statistics-report/index.html
- M.E. Piyasena, S.W. Graves, The intersection of flow cytometry with microfluidics and microfabrication. Lab Chip 14(6), 1044–1059 (2014)
- S.R. Quake, A. Scherer, From micro-to nanofabrication with soft materials. Science 290(5496), 1536–1540 (2000)
- D.R. Reyes, D. Iossifidis, P.-A. Auroux, A. Manz, Micro total analysis systems. 1. introduction, theory, and technology. Anal. Chem. 74(12), 2623–2636 (2002)
- G.T. Smith, N. Dwork, S.A. Khan, M. Millet, K. Magar, M. Javanmard, A.K.E. Bowden, Robust dipstick urinalysis using a low-cost, microvolume slipping manifold and mobile phone platform. Lab Chip 16(11), 2069–2078 (2016)
- J. Sui, F. Foflonker, D. Bhattacharya, M. Javanmard, Electrical impedance as an indicator of microalgal cell health. Sci. Rep. 10(1), 1251 (2020)
- J. Sui, P. Xie, Z. Lin, M. Javanmard, Electronic classification of barcoded particles for multiplexed detection using supervised machine learning analysis. Talanta 215, 120791 (2020)
- S. Talebian, M. Javanmard, Compact and automated particle counting platform using smartphone-microscopy. Talanta 228, 122244 (2021)



43 Page 10 of 10 Biomedical Microdevices (2023) 25:43

M.H. Tania, K.T. Lwin, A.M. Shabut, M. Najlah, J. Chin, M.A. Hossain, Intelligent image-based colourimetric tests using machine learning framework for lateral flow assays. Expert Syst. Appl. 139, 112843 (2020)

- M. Tayyab, P. Xie, M.A. Sami, H. Raji, Z. Lin, Z. Meng, S.R. Mahmoodi, M. Javanmard, A portable analog front-end system for label-free sensing of proteins using nanowell array impedance sensors. Sci. Rep. 12(1), 20119 (2022)
- S. Wang, F. Xu, U. Demirci, Advances in developing hiv-1 viral load assays for resource-limited settings. Biotechnol. Adv. 28(6), 770–781 (2010)
- D.B. Weibel, W.R. DiLuzio, G.M. Whitesides, Microfabrication meets microbiology. Nat. Rev. Microbiol. 5(3), 209–218 (2007)
- G.M. Whitesides, The origins and the future of microfluidics. Nature **442**(7101), 368–373 (2006)
- Y. Xia, J. Si, Z. Li, Fabrication techniques for microfluidic paper-based analytical devices and their applications for biological testing: A review. Biosens. Bioelectron. 77, 774–789 (2016)
- P. Xie, N. Song, W. Shen, M. Allen, M. Javanmard, A ten-minute, single step, label-free, sample-to-answer assay for qualitative detection of cytokines in serum at femtomolar levels. Biomed. Microdevices 22, 1–9 (2020)
- P. Yager, T. Edwards, E. Fu, K. Helton, K. Nelson, M.R. Tam, B.H. Weigl, Microfluidic diagnostic technologies for global public health. Nature 442(7101), 412–418 (2006)
- H. Yu, Y. Lu, Y.-G. Zhou, F.-B. Wang, F.-Y. He, X.-H. Xia, A simple, disposable microfluidic device for rapid protein concentration and purification via direct-printing. Lab Chip 8(9), 1496–1501 (2008)

- J.Y. Zhang, J. Do, W.R. Premasiri, L.D. Ziegler, C.M. Klapperich, Rapid point-of-care concentration of bacteria in a disposable microfluidic device using meniscus dragging effect. Lab Chip 10(23), 3265–3270 (2010)
- Y. Zhang, Y. Zhao, T. Cole, J. Zheng, J. Guo, S.-Y. Tang et al., Micro-fluidic flow cytometry for blood-based biomarker analysis. Analyst 147(13), 2895–2917 (2022)
- L. Zhang, H. Zhang, Q. Xie, S. Xiong, F. Jin, F. Zhou, H. Zhou, J. Guo, C. Wen, B. Huang et al., A bibliometric study of global trends in diabetes and gut flora research from 2011 to 2021. Front. Endocrinol. 13, 990133 (2022)
- W. Zhao, S. Tian, L. Huang, K. Liu, L. Dong, J. Guo, A smartphone-based biomedical sensory system. Analyst 145(8), 2873–2891 (2020)
- B. Zhou, Y. Lu, K. Hajifathalian, J. Bentham, M. Di Cesare, G. Danaei, H. Bixby, M.J. Cowan, M.K. Ali, C. Taddei et al., Worldwide trends in diabetes since 1980: a pooled analysis of 751 populationbased studies with 4 · 4 million participants. Lancet 387(10027), 1513–1530 (2016)

Publisher's Note Springer Nature remains neutral with regard to jurisdictional claims in published maps and institutional affiliations.

Springer Nature or its licensor (e.g. a society or other partner) holds exclusive rights to this article under a publishing agreement with the author(s) or other rightsholder(s); author self-archiving of the accepted manuscript version of this article is solely governed by the terms of such publishing agreement and applicable law.

